Cell Tissue Res (2002) 310:279–287
DOI 10.1007/s00441-002-0644-6

REGULAR ARTICLE

**S. Ständer · H. G. Bone · H. G. Machens · T. Aberle
W. Burchard · T. Prien · T. A. Luger · D. Metze**

Hydroxyethyl starch does not cross the blood-brain or the placental barrier but the perineurium of peripheral nerves in infused animals

Received: 11 June 2002 / Accepted: 16 September 2002 / Published online: 5 November 2002

Abstract Therapy with hydroxyethyl starch (HES) is associated with a high incidence of persistent pruritus due to HES storage in cutaneous nerves. Up to now it has been unknown if HES also accumulates in the extracutaneous peripheral or central nervous system. To study this, five rats including one pregnant one were infused with a single dose (34–150 mg) of HES (70/200/450 kDa molecular weight) conjugated with fluorescein isothiocyanate (FITC). In addition, four sheep were infused with a cumulative dosage of 30 g, 120 g, and 420 g HES (200 kDa), respectively. After 7–13 days, biopsies from the adult rats, four fetal rats and sheep were taken from various organs. The specimens were analyzed by light, electron, and confocal laser scanning microscopy. Typical HES storage vacuoles were found in macrophages of the skin, liver, spleen, lung, and kidney. HES storage in healthy animals was not associated with signs of either inflammation or apoptosis contrary to a previously described animal hemorrhagic shock model. Beyond that, fetus biopsies did not show any storage phenomenon, confirming that HES does not cross the placental barrier. Deposits of HES could be detected in Schwann cells of cutaneous nerve fibers as well as in perineural and endoneural cells of sciatic nerve in one rat (HES 450 kDa) and three of four sheep. No HES storage was found in the central nervous system. Our findings clearly demonstrate that storage of HES is detectable only in small peripheral nerves, suggesting a cutaneous origin of the HES-induced pruritus.

Keywords Hydroxyethyl starch · Pruritus · Nerve fibers · Blood-brain barrier · Placental barrier · Rat (Sprague Dawley) · Sheep

S. Ständer (✉) · T.A. Luger · D. Metze
Department of Dermatology and Ludwig Boltzmann Institute for Cell Biology and Immunobiology of the Skin, University of Münster, Münster, Germany
e-mail: sonja.staender@uni-muenster.de
Tel.: +49-251-8356504, Fax: +49-251-8356522

H.G. Bone · T. Prien
Department of Anesthesiology and Intensive Care Medicine, University of Münster, Münster, Germany

H.G. Machens
Clinic for Plastic, Hand and Reconstructive Surgery, Hannover Medical School, Hannover, Germany

T. Aberle · W. Burchard
Institute of Macromolecular Chemistry, University of Freiburg, Freiburg, Germany

S. Ständer
Department of Dermatology, University of Münster, Von-Esmarchstrasse 58, 48149 Münster, Germany

Introduction

Hydroxyethyl starch (HES) is widely used as a plasma substitute and for improvement of the microcirculation (Hulse and Jacobi 1983). For a number of years HES has proved to be a save and efficient hemodilution therapy of otological disorders, peripheral arterial stenosis, cerebral and cardial ischemia, and hypoperfusion of the retina or the placenta (Messmer et al. 1986; Kiesewetter et al. 1990; Leunig et al. 1995). In addition, HES is used during autologous blood transfusion and hemodialysis, for the prevention of postoperative thrombosis, as a sedimenting agent during leukapheresis and as a priming fluid in extracorporal units (Richter and Hedin 1983; Förster 1989). In contrast to dextran preparations, serious side effects, such as anaphylactic reactions, occur only rarely (Kraft et al. 1992). However, in the past few years several authors have reported a high incidence of a persistent and severe pruritus associated with HES administration (Parker et al. 1982; Gall et al. 1993; Jurecka et al. 1993; Metze et al. 1997; Murphy et al. 2001; Kimme et al. 2001). Moreover, tissue storage of HES has often been demonstrated in various organs including the skin of rodents and humans (Parth et al. 1992; Jurecka et al. 1993; Metze et al. 1997; Sirtl et al. 1999; Ständer et al. 2001) and could also be found in cutaneous nerves in patients suffering from pruritus (Metze et al. 1997; Ständer et al. 2001). Storage of HES in Schwann cells of unmyelinated axons constituting sensory C-fibers has

been postulated to directly induce itching by influencing neuronal functions. Since it is known that itch perception can be modified on various levels of the peripheral and central nervous system, it was questionable whether HES also influences the extracutaneous itch cognition. Accordingly, the aim of our current study was to determine in an animal model whether HES administration of different dosage and HES preparations also leads to storage in extracutaneous peripheral nerves and the central nervous system. Since HES storage has been described previously in the placenta of infused pregnant women, it seemed to be of particular interest to investigate whether HES crosses the placental barrier and is stored in fetal tissue. Furthermore, since HES was reported to significantly increase the rate of apoptosis in lung, several tissues were investigated for apoptosis.

Materials and methods

Preparation of FITC-labeled HES

HES preparations were made following a slightly modified method as described by DeBelder and Granath (1973): 1.19 g HES (dried at 70°C over P_2O_5 in oil pump vacuum) was added to 15 ml dimethylsulfoxide (DMSO) and heated at 95°C. After the HES was fully dissolved, 125 mg fluorescein isothiocyanate (FITC, Sigma, Taufkirchen, Germany) was added. After 6 h the solution was cooled to room temperature and added to 100 ml ethanol, to precipitate the labeled HES. To get rid of any free unreacted FITC, the precipitated HES was dissolved in 20 ml deionized water and dialysed against water for several days. The exclusion volume of the membrane was 3,500 g/mol. Final isolation of the labeled HES was done by freeze drying. The degree of substitution (DS) was maximum, DS=0.02.

Animals

All animal experiments were performed according to Lower Saxony Law regarding the protection of laboratory animals and were approved by the State Animal Protection Committees. Animal studies were performed in two parts. In a pilot trial, two rats and two sheep were infused and some tissues were analyzed to prove the validity of the method. After that, animals were subjected to different infusion protocols and a larger series of tissues was studied. Due to the induced hypervolemia and resulting side-effects such as hypertension in healthy animals, rats can only be infused with a low HES dosage while sheep also tolerate higher dosages. Accordingly, the rats received HES of different molecular weights at a low HES dosage and the sheep could be infused with different HES dosages and time points of biopsy while receiving one HES preparation only.

Five healthy rats (female Sprague-Dawley, 100–375 g, Table 1) were infused once via the tail vein with different HES preparations (70 kDa, 200 kDa, 450 kDa) and different HES dosages (27–150 mg). One rat receiving 34 mg HES 70 kDa/0.02 DS was pregnant (four fetuses, age estimate 17 days). For proper conformation that the observed storage phenomena are related to HES, rats 2–5 were infused with FITC-labeled HES. As negative controls, one rat received unlabeled HES and another rat was not infused. All rats were killed 12 days after HES infusion by ether inhalation. Back skin, liver, spleen, lung, sciatic nerve, and brain (including gray and white zones) were biopsied.

Four healthy sheep (female sheep of the merino breed, mean body weight 45 kg, Table 2) were slowly infused with HES of different cumulative dosage. The sheep received a daily infusion of 500 ml 6% HES 200 kDa with a degree of substitution (SD) of 0.5 intravenously in the jugular vein once (n=1), four (n=1) or 14 (n=2) times, respectively. Seven, 10 and 14 days after HES infusions, sheep were anesthetized and killed with a lethal dose of potassium chloride. Biopsies from the skin of the back, liver, spleen, kidney, sciatic nerve, and brain (both gray and white zones) were obtained. As control, the same tissues from a non-infused sheep were investigated.

Tissue processing and staining procedures

All biopsies such as skin, liver, spleen, sciatic nerve, and brain from both rats and sheep, as well as lung from rats and kidney from sheep (Tables 1, 2), were divided and processed for either light- or electron-microscopic examinations. One part was fixed in Karnovsky's fixative, postfixed in 1% osmium tetroxide, dehydrated, and embedded in Epon. Semithin sections were cut with glass knives on an ultramicrotome (OMU3, Reichert-Jung, Vienna, Austria) and stained with toluidine blue. For electron microscopy, ultrathin sections were cut with diamond knives, mounted on copper grids, and stained with uranyl acetate and lead citrate. All of the ultrathin preparations were examined under a Philips CM10 electron microscope (Kassel, Germany).

The second part of the biopsies was fixed in 7% buffered formalin, embedded in paraffin and stained with hematoxylin-eosin (HE). A nick-end labeling technique (terminal deoxynucleotidyl transferase-mediated dUTP nick-end labeling, TUNEL) was performed to visualize apoptotic cell death at the single cell level. For this, paraffin sections were nick-end labeled with biotinylated deoxyuridine (dU) introduced by terminal deoxytransferase (TαT), and then stained using avidin-conjugated peroxidase. The protocol and reagents as described by Gavrieli et al. (1992) were used. Light-microscopic investigations of the paraffin specimens and semithin sections were performed on a Zeiss-Axioplan microscope (Cologne, Germany).

Skin, liver, spleen, lung, peripheral nerve and brain biopsies of FITC-labeled and unlabeled HES-infused rat were immediately

Table 1 Experimental regime of infused rats (*S* skin, *L* liver, *Sp* spleen, *Lg* lung, *N* sciatic nerve, *B* brain)

Rat/body weight (bw)	Molecular weight (MW) and degree of substitution (DS) of HES	Cumulative dosage/number of administrations	Timepoint of biopsy after infusion	Investigated tissues
No. 1/250 g	MW 200 kDa, DS 0.5, unlabeled	150 mg HES (1 ml/100 g body weight)/1	After 12 days	S, L, Sp
No. 2/100 g	MW 200 kDa, DS 0.02, FITC-labeled	60 mg (1 ml/100 g bw)/1	After 12 days	S, L, Sp
No. 3/300 g	MW 200 kDa, DS 0.02, FITC-labeled	27 mg (0.15 ml/100 g BW)/1	After 12 days	S, L, Sp, Lg, N, B
No. 4/300 g	MW 450 kDa, DS 0.02, FITC-labeled	27 mg (0.15 ml/100 g BW/1	After 12 days	S, L, N, B
No. 5/375 g	MW 70 kDa, DS 0.02, FITC-labeled	34 mg (0.15 ml/100 g BW/1	After 12 days	S, L, N, B
No. 6	Not infused	–	–	S, L, Sp, N, B
Nos. 7–10: fetuses of rat no. 5	MW 70 kDa, DS 0.02, FITC-labeled	Mother 34 mg/1	After 12 days	S, L, B

Table 2 Experimental regime of infused sheep (*S* skin, *L* liver, *Sp* spleen, *K* kidney, *N* sciatic nerve, *B* brain)

Sheep	Molecular weight (MW) and degree of substitution (DS) of HES	Cumulative dosage/number of administrations (30 g each)	Timepoint of biopsy after last infusion	Investigated tissues
No. 1	MW 200 kDa, DS 0.5	30 g HES (0.7 g/kg bw)/1	After 7 days	S, L
No. 2	MW 200 kDa, DS 0.5	120 g (2.7 g/kg bw)/4	After 13 days	S, L, Sp, N
No. 3	MW 200 kDa, DS 0.5	420 g (9.3 g/kg bw)/14	After 7 days	S, L, Sp, K, N, B
No. 4	MW 200 kDa, DS 0.5	420 g (9.3/kg bw)/14	After 10 days	S, L, Sp, K, N, B
No. 5	Not infused	–	–	S, L, Sp, N, B

frozen in liquid nitrogen at –80°C. Frozen sections were cut and mounted on coated slides. Sections were immediately investigated with a Zeiss Axioplan 100-W HBO fluorescence microscope emitting UV light at a wavelength of 450–490 nm. In addition, the specimens were investigated with a confocal laser scanning microscope equipped with an argon laser (Wild Leitz-CLSM Diaplan, Leitz, Heidelberg, Germany). Sections of 0.005–0.05 mm thickness were x/y scanned in the reflecting mode. For optical sectioning, the pinhole was closed to 125 nm and image averaging was performed. The images were stored on an optic disk, later processed with a highpass filter using extended focus mode and displayed in glow overflow pseudocolor.

Results

Light microscopy

The gross morphology of the organs in HES-infused animals, both rats including fetus and sheep, appeared not to be affected. In routine hematoxylin-eosin-stained paraffin-embedded specimens, no signs of inflammation, intra- or extracellular edema or intracytoplasmic vacuolization were visible as compared to tissues of non-infused animals. Furthermore, no signs of apoptosis and apoptotic cells were detectable, e.g., shrunken cells with pyknotic nuclei and eosinophilic cytoplasm. The in situ hybridization TUNEL method, which is described to be sensitive for labeling apoptotic nuclei in tissues, failed to show abnormal staining of various investigated organs, whereas a positive control of human skin tissue (erythema multiforme) revealed abundant staining of DNA fragmentation (Chrysomali et al. 1997) (Fig. 1d, e).

Fluorescence microscopy in rats

Fluorescence and confocal laser scanning microscopy was performed in rats infused with FITC-labeled HES demonstrating marked green fluorescence in various organs. In the liver of all animals an intense granular fluorescence of dendritic Kupffer cells as found in hepatic sinusoids became evident (Fig. 1b). The lipofuscin granules of the liver showed a brown-yellow color which could easily be distinguished from green FITC fluorescence. The spleen showed a granular fluorescence in macrophages of lymph follicles surrounding the central artery within the white spleen pulp (Fig. 1a). Granular fluorescence was also detectable in macrophages of the lung. In the skin, green fluorescence was visible in macrophages with much lower intensity than in liver and spleen (Fig. 1c). However, no fluorescence was detectable in cutaneous endothelial cells, nerve fibers, adnexal structures and epidermal keratinocytes. Overall, the fluorescence distribution was nearly the same in all infused rats without remarkable differences with regard to the molecular weight of the infused HES ranging from 70 kDa to 450 kDa. In sciatic nerves, a weak fluorescence intensity could be found mainly in the perineurium. However, no fluorescence was found in the white and gray zone of the central nervous system. Furthermore, in fetal skin, liver, and brain no fluorescence was detectable. As negative control, biopsies of one rat infused with unlabeled HES and one non-infused rat were investigated. No fluorescence was detectable in the investigated tissues such as skin, liver, spleen, peripheral nerve and brain.

Electron microscopy

A characteristic intracytoplasmic vacuolization of macrophages of various investigated tissues was a regular finding in both infused rats and sheep (Figs. 2c, 3a). In semithin sections clear vacuoles with a distinct marginal bluish content were invariably visible in the cytoplasm of macrophages at light-microscopic level. At the ultrastructural level, electron-lucent intracytoplasmic vacuoles lined by a unit cell membrane were obvious. Interestingly, vacuoles as found in sheep revealed electron-dense amorphous material at the periphery (Fig. 3a, c, e), whereas in rats only a few vacuoles showed this phenomenon (Fig. 2a, c). The vacuoles, though they vary in content of amorphous material, were comparable to those previously described in human cutaneous macrophages (Metze et al. 1997; Ständer et al. 2001). Non-infused control animals regularly lacked intracytoplasmic vacuolization in the investigated tissues.

Rats revealed intracytoplasmic vacuolization of macrophages in spleen, liver, lung, and skin (Fig. 2c). The degree of vacuolization in each biopsy was estimated by comparing the number and size of vacuoles in the macrophages. Differences in the degree of vacuolization were not evident despite different HES preparations. In cutaneous endothelial cells, distinct vacuolization could be found while cutaneous keratinocytes and adnexal epithelial cells were consistently normal. In cutaneous nerve fibers, vacuoles could be found in the cytoplasm of

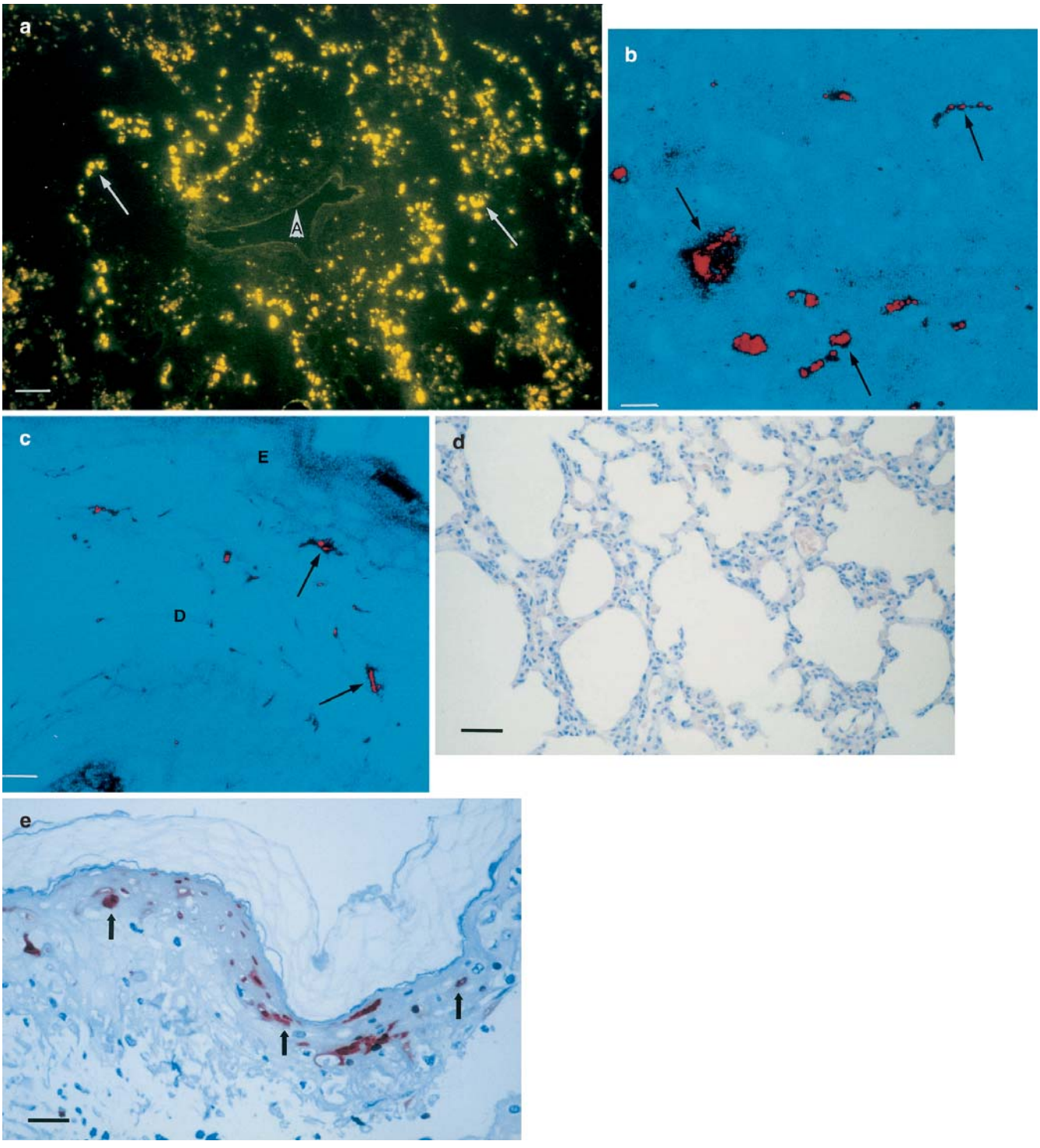

Fig. 1 **a** Fluorescence microscopy demonstrating a granular green fluorescence (*arrows*) in resident macrophages within a lymph follicle in the white spleen pulp of rat, representing HES storage of an FITC-labeled HES (MW 70 kDa)-infused rat. Artery (*A*) in the center of a lymph follicle. **b, c** Confocal laser scanning microscopy of rat liver (**b**) and skin (**c**) (*E* epidermis, *D* dermis). FITC-labeled HES is detectable in resident macrophages (*arrows*). Fluorescence is shown in green (**a**) and red pseudocolors (**b, c**). **d, e** Detection of apoptotic cell death by the TUNEL technique. In rat lung no DNA fragmentation could be found (**d**). As positive control served a skin biopsy of erythema multiforme with multiple apoptotic cells (*arrows*) in the epidermis (**e**). *Scale bars* 52 µm (**a**), 27 µm (**b, e**), 19 µm (**c, d**)

a Schwann cell in large myelinated nerve fibers (Fig. 2a) from one rat infused with HES of high molecular weight (450 kDa). In the sciatic nerve of rats, vacuolization of perineural cells due to HES was doubtful (Fig. 2b), while Schwann cells of the nerve fibers clearly showed no vacuolization. Moreover, in the white and gray zone of the central nervous system no HES storage was detectable (Fig. 2d). Of particular interest, tissues of fetal rats such as skin, liver and brain did not show any signs of intracytoplasmic vacuolization (Fig. 2e).

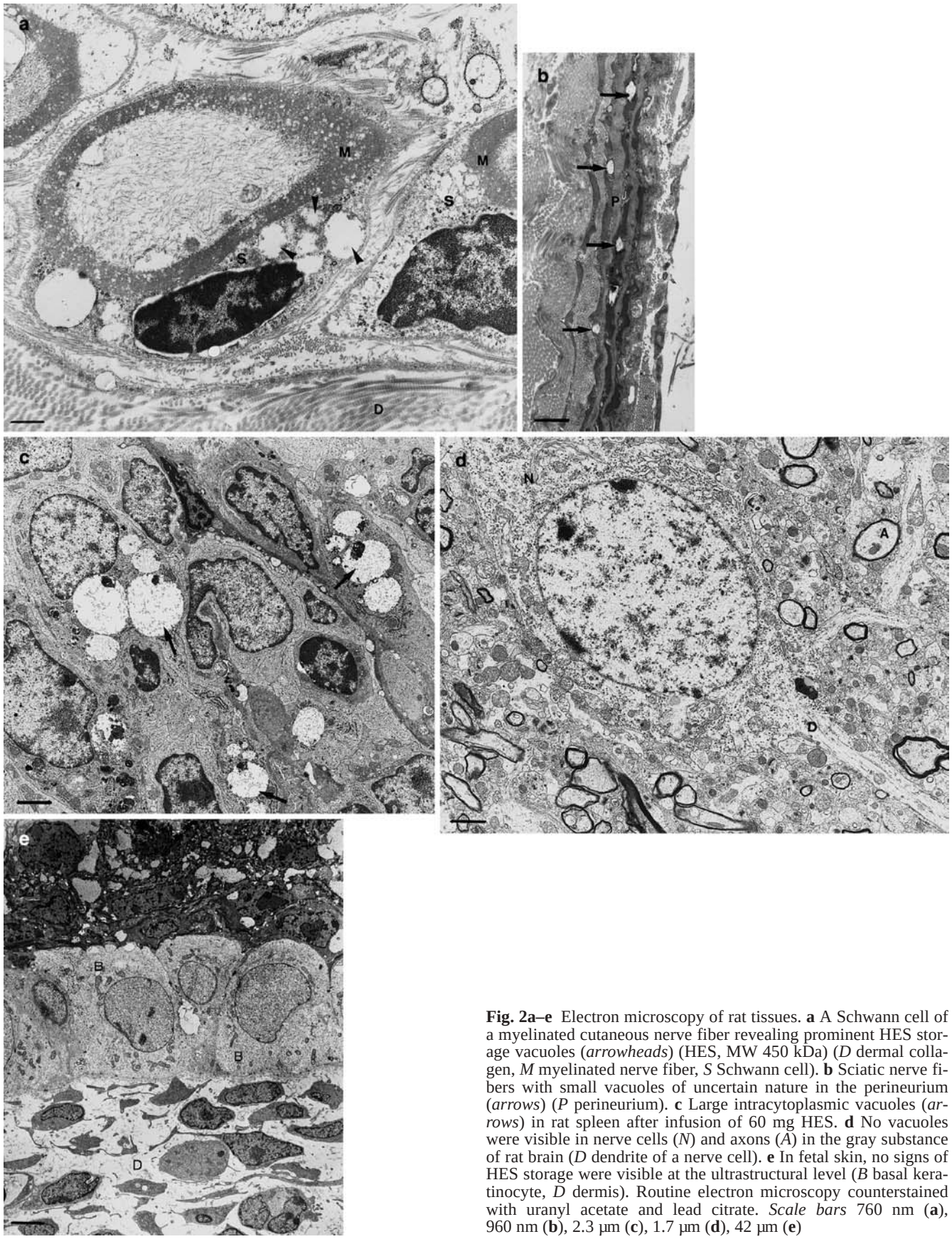

Fig. 2a–e Electron microscopy of rat tissues. **a** A Schwann cell of a myelinated cutaneous nerve fiber revealing prominent HES storage vacuoles (*arrowheads*) (HES, MW 450 kDa) (*D* dermal collagen, *M* myelinated nerve fiber, *S* Schwann cell). **b** Sciatic nerve fibers with small vacuoles of uncertain nature in the perineurium (*arrows*) (*P* perineurium). **c** Large intracytoplasmic vacuoles (*arrows*) in rat spleen after infusion of 60 mg HES. **d** No vacuoles were visible in nerve cells (*N*) and axons (*A*) in the gray substance of rat brain (*D* dendrite of a nerve cell). **e** In fetal skin, no signs of HES storage were visible at the ultrastructural level (*B* basal keratinocyte, *D* dermis). Routine electron microscopy counterstained with uranyl acetate and lead citrate. *Scale bars* 760 nm (**a**), 960 nm (**b**), 2.3 μm (**c**), 1.7 μm (**d**), 42 μm (**e**)

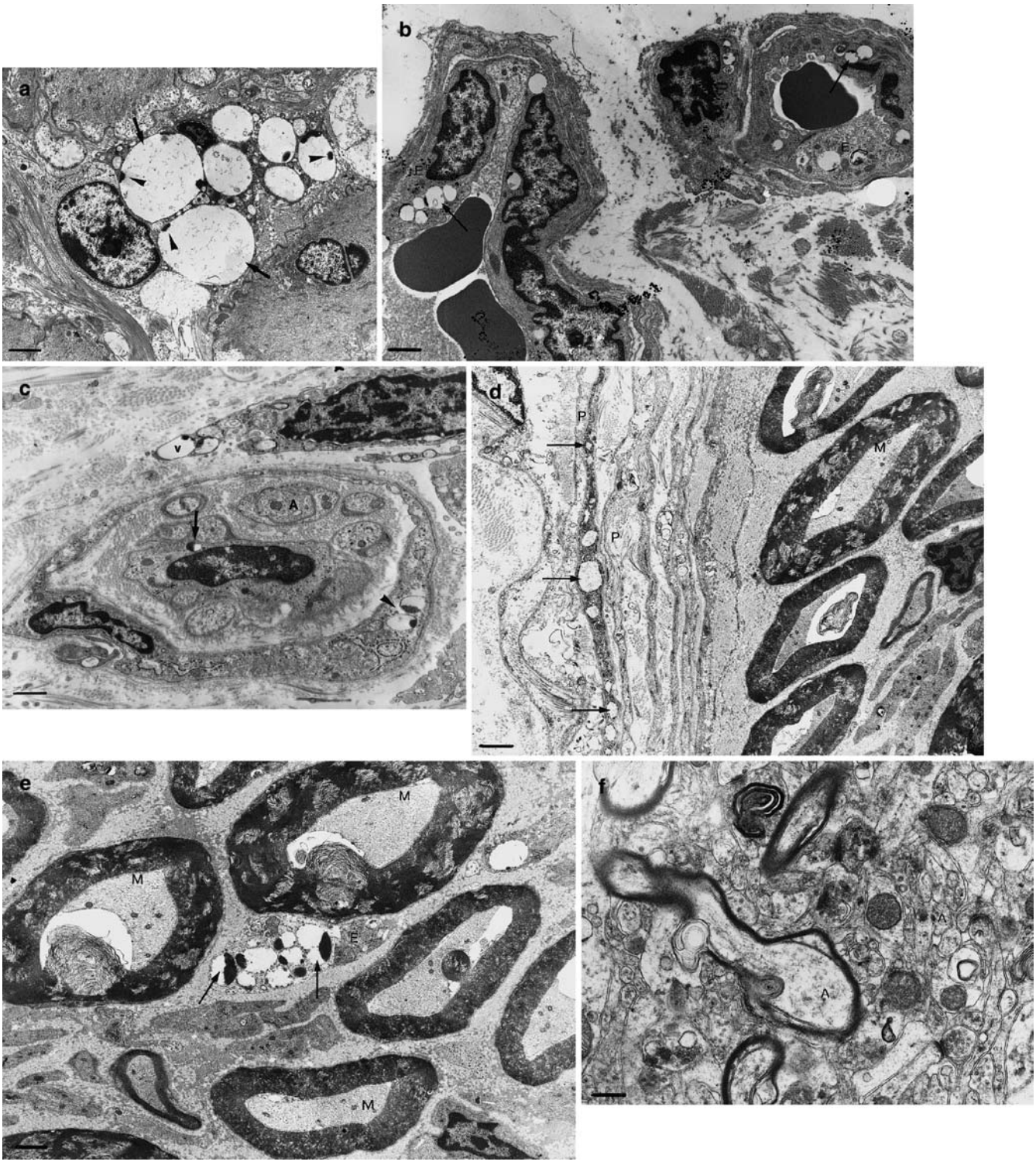

Fig. 3a–f Electron microscopy of sheep tissues. **a** Large intracytoplasmic vacuolization (*arrows*) with focal amorphous material (*arrowheads*) in dermal macrophages of HES-infused sheep. **b** Small HES vacuoles (*arrows*) in endothelial cells (*E*) of dermal vessels. **c** Storage vacuoles could be demonstrated in Schwann cells (*arrow*) and perineurium (*arrowhead*) of unmyelinated cutaneous nerve fibers (*A* axon, *v* vacuoles in a dermal macrophage). **d, e** Extracutaneous sciatic nerve revealed small vacuoles (*arrows*) in **d** perineural (*P*) and **e** endoneural cells (*E*) between myelinated axons (*M*). **f** No vacuoles were visible in the white substance of infused sheep (*A* myelinated and unmyelinated axon). Routine electron microscopy counterstained with uranyl acetate and lead citrate. *Scale bars* 1.5 μm (**a**), 1.3 μm (**b, e**), 960 nm (**c**), 430 nm (**f**), 1.7 μm (**d**)

In all infused sheep large intracytoplasmic vacuoles were a consistent finding in macrophages of the skin (Fig. 3a), liver, spleen and kidney. Interestingly, a variation in the degree of vacuolization in cutaneous macrophages could be observed. In animals which had received 30 g or 120 g, the number and size of vacuoles appeared to be lower than in sheep infused with 420 g. Endothelial cells of cutaneous vessels revealed small vacuoles in all sheep (Fig. 3b) while keratinocytes were consistently normal. Adnexal epithelia of sweat glands and hair follicles revealed vacuoles only in two sheep that received high HES dosages. Sebaceous glands regularly appeared devoid of HES-related vacuoles. In Schwann cells of cutaneous myelinated and unmyelinated nerve fibers, abundant vacuolization was obvious in the sheep infused with 420 g HES (sheep No. 4, 420 g HES, biopsy after 10 days, Fig. 3c). In the other sheep infused with 420 g (sheep No. 3, 420 g HES, biopsy after 7 days) as well as in the sheep infused with 120 g, vacuolization was confined to large myelinated cutaneous nerve fibers. No cutaneous neuronal HES storage could be detected in the sheep infused with 30 g HES.

All of the sciatic nerves of sheep investigated revealed clear vacuoles of different size in endoneural phagocytic cells and in the perineural layers while Schwann cells of both myelinated and unmyelinated nerve fibers revealed no storage vacuoles (Fig. 3d, e). Likewise, no storage of HES was found in the white and gray zone of the central nervous system in the studied sheep. In the gray zone, all nerve cells were regular. In the white zone, characterized by lots of nerve axons and surrounding oligodendroglia cells, no vacuoles could be demonstrated (Fig. 3f). The phagocytic microglia cells in both the white and gray zone lacked vacuolization.

Discussion

The colloid plasmaexpander hydroxyethyl starch (HES) consists of ethylated glucose units with high water-binding capacity. After intravenous administration, HES is degraded by intravascular α-amylase, and eliminated by renal clearance or intracellular lysosomal uptake (Thompson et al. 1979). Intracellular HES uptake results in transient tissue storage and consecutive degradation by lysosomal α-glucosidase. HES storage could previously be demonstrated immunohistochemically in various organs including the skin of rodents and humans (Parth et al. 1992; Jurecka et al. 1993; Metze et al. 1997; Sirtl et al. 1999; Förster et al. 1999; Ständer et al. 2001). Beyond that, intracytoplasmic HES storage could be directly visualized in previous animal studies applying FITC-labeled HES. Fluorescence was detectable in macrophages as early as 180 min after HES infusion (Förster et al. 1999). In the present study, all rats infused with FITC-labeled HES demonstrated intense to weak fluorescence in many tissues such as liver, spleen, lung, peripheral nerve and skin. Tissue storage of HES was further characterized by typical ultrastructural features. Electron microscopy demonstrated electron-lucent lysosomal storage vacuoles with marginal amorphous material in cutaneous macrophages, endothelial cells, keratinocytes, and sweat glands in humans (Metze et al. 1997; Ständer et al. 2001) as well as in macrophages of liver, spleen, lung, lymph nodes, and kidney from infused animals (Parth et al. 1992; Jurecka et al. 1993). By means of immunoelectron microscopy, reactivity for HES could be proven in the amorphous material and along the wall of the vacuoles (Metze et al. 1997; Ständer et al. 2001). In the present investigation, typical HES-associated intracytoplasmic vacuoles could be found in macrophages in the skin, liver, spleen, kidney, lung, and peripheral nerve of infused animals. Fluorescence and electron microscopy revealed comparable results in this study. Moreover, the latter proved to have more sensitivity, also detecting minimal HES storage in small vacuoles as found in endothelial cells and nerve fibers of rat skin which could not be seen by fluorescence microscopy. Interestingly, compared to HES vacuoles of human skin, HES-related storage vacuoles of investigated rats revealed less amorphous material possibly due to a variation in the tissue metabolism.

It has been shown in previous studies that the degree of macrophage HES storage correlates with both the cumulative HES dosage and the time point of biopsy after HES administration, but less with the molecular weight (MW) of the HES preparation (Metze et al. 1997; Ständer et al. 2001). To evaluate both the degree of vacuolization and the influence of the HES preparation, different infusion regimes were selected. Rats which can be infused with low HES dosage only, therefore received HES of different MW (MW 70/200/450 kDa) and of almost the same HES dosage. Only the first two rats were infused with a higher HES dosage for better evaluation of FITC-labeled HES fluorescence intensity. Various rat tissues showed nearly the same distribution of HES vacuoles, again suggesting that the given HES preparation had no influence on the degree of vacuolization. Sheep, which are known to tolerate higher HES dosages, received one HES preparation (MW 200 kDa) with different HES dosage and time points of biopsy. As expected, distribution of HES vacuoles in skin biopsies suggests a dosage- and time-point-dependent accumulation of HES in dermal macrophages and adnexal epithelial cells. Though results were obtained from single animals only, they are consistent with findings in humans and again underline the fact that the skin is regularly involved in the storage and the metabolism of HES (Metze et al. 1997; Ständer et al. 2001).

In general, intracellular storage of HES in macrophages and epithelial cells does not lead to any adverse effects. For example, renal tubules of infused animals revealed abundant swelling while renal function was shown to be regular (Thompson et al. 1979). Furthermore, though HES storage is most extensive in macrophages, the mononuclear phagocytic system (MPS) function is not impaired (Shatney and Chandry 1984; White et al. 1986). Moreover, some authors stated that the func-

tion of the MPS is improved after HES administration (Lenz et al. 1986). Recently, Deb et al. reported significantly increased apoptosis after HES administration in a hemorrhagic shock rat model (Deb et al. 2000). Apoptosis was detected in blood cells and lung of infused animals as demonstrated by TUNEL assay and bax protein expression, a member of the Bcl-2 family and an important regulator of the programmed cell death (Knudson and Korsmeyer 1997). However, in our study, investigated tissues especially the lung of healthy infused animals revealed no signs of DNA fragmentation. Accordingly, it seems likely that the previously described HES-induced apoptosis is an additive effect in preformed tissue damage and is not related to HES administration per se.

Of further interest, HES infusion therapy was described to be effective in pregnant patients suffering from plasma volume contraction, fetal growth weight retardation and preeclampsia (Heilmann 1989). However, placental lysosomal HES storage has been described after infusion therapy (Heilmann 1989; Heilmann et al. 1991; Saling et al. 1990; Unger et al. 1990). Though no starch could be found in the umbilical cord blood (Heilmann 1989), it has so far been unclear whether HES passes the placental barrier with possible hemodynamic risk to the fetus. In our study, a pregnant rat was infused. Neither in the skin, liver nor central nervous system of four fetuses were storage phenomena detectable, suggesting that HES does not cross the placental barrier. Since we observed results in one pregnant rat only, further studies with a larger group are necessary to demonstrate that HES is a safe plasma expander in pregnancy. However, these results are congruent with a clinical trial demonstrating that HES infusion therapy had only minimal effects on fetal myocardial performance and no effect on the clinical conditions of newborns (Karinen et al. 1994), suggesting that HES develops most of its hemodynamic effects on the maternal side of the placenta.

The main side-effect of HES infusion therapy is a severe generalized or localized pruritus directly correlated with higher cumulative dosage exceeding 200 g HES (Gall et al. 1993, 1996; Leunig et al. 1995; Metze et al. 1997; Murphy et al. 2001; Kimme et al. 2001). In previous morphological studies, pruritus could be related to HES storage in Schwann cells of cutaneous myelinated and unmyelinated nerves (Metze et al. 1997). Since it is known that pruritus is perceived and modulated at various levels of the peripheral and central nervous system (Schmelz 2001), the aim of the present study was to further clarify the origin of this type of pruritus. As expected, administration of higher cumulative dosages resulted in HES storage in Schwann cells of cutaneous nerve fibers of sheep. Interestingly, a larger number of nerve fibers showed vacuolization with higher HES dosage and a later time point of biopsy. These results are consistent with neuronal HES storage in patients with pruritus (Metze et al. 1997). In rats, only one animal infused with a low dosage of high molecular weight HES (Mw 450 kDa) revealed a clear vacuolization in Schwann cells of cutaneous nerve fibers, while all other rats' nerve fibers were unaffected. This is surprising, since to date only high cumulative HES dosages independent of molecular weight were assumed to be associated with HES uptake in cutaneous nerve fibers (Metze et al. 1997).

Large extracutaneous nerves revealed clear vacuoles after administration of HES. In sheep, prominent HES storage vacuoles could be detected in both perineural and endoneural cells, but not in Schwann cells of sciatic nerves, after administration of a cumulative dosage exceeding 120 g. In contrast, small HES vacuoles were suspected in perineural layers but clearly absent in endoneural phagocytic or Schwann cells of sciatic nerves in all HES infused rats. In the central nervous system of all infused animals, no HES-related storage phenomena could be detected in different brain areas. The consistent absence of HES storage in the brain is of further interest. In previous animal studies, HES-infused rats and cats revealed significantly less brain tissue necrosis after cerebral trauma and ischemia than control animals, suggesting improved perfusion of the salvageable brain tissue surrounding the core injury (Chorny et al. 1999; Sakaki et al. 1990). However, brain water content was not increased, suggesting that HES does not pass the blood-brain barrier and has no effect on intracerebral liquids (Eilig et al. 2001). Furthermore, HES itself could be demonstrated to prevent disruption of the blood-brain barrier and reduce vascular permeability by action on endothelial junctions (Schell et al. 1992; Zikria et al. 1989; Chi et al. 1996). Our study provides direct evidence that HES does not cross the blood-brain barrier at least in animals with an intact anatomy of the barrier.

In sum, our results favor the idea that HES storage in different compartments of extracutaneous peripheral nerves may be an additional phenomenon of transient tissue storage. Since Schwann cells of sciatic nerves are not involved in the storage of HES, it seems unlikely that HES storage in extracutaneous nerves plays a role in the etiopathology of HES-induced pruritus. In conclusion, our studies suggest a cutaneous origin of the HES-induced pruritus which could explain the clinical characteristics of the symptoms. The episodic itch following HES therapy is recurrently triggered by friction, a phenomenon known as allokinesis. This form of localized pruritus is provoked by non-pruritic stimuli due to a dysfunction of cutaneous nerve fibers. In addition, the cutaneous neurogenic origin of the HES pruritus would also account for the inefficacy of antihistamines and the response to topical anesthetics and capsaicin (Szeimies et al. 1994; Metze et al. 1997).

Acknowledgements The technical assistance of A. Wissel, C. Focke, C. Post, and J. Crout and the excellent micrographic work of P. Wissel and J. Bückmann is gratefully acknowledged.

References

Chi OZ, Lu X, Wei HM, Williams JA, Weiss HR (1996) Hydroxyethyl starch solution attenuates blood-brain barrier disruption caused by intracarotid injection of hyperosmolar mannitol in rats. Anesth Analg 83:336–341

Chorny I, Bsorai R, Artru AA, Talmor D, Benkoviz V, Roytblat L, Shapira Y (1999) Albumin or hetastarch improves neurological outcome and decreases volume of brain tissue necrosis but not brain edema following closed-head trauma in rats. J Neurosurg Anesthesiol 11:273–281

Chrysomali E, Lozda-Nur F, Dekker NP, Papanicolaou SI, Regezi JA (1997) Apoptosis in oral erythema multiforme. Oral Surg Oral Med Oral Pathol Oral Radiol Endod 83:272–280

Deb S, Sun L, Martin B, Talens E, Burris D, Kaufmann C, Rich N, Rhee P (2000) Lactated Ringer's solution and hetastarch but not plasma resuscitation after rat hemorrhagic shock is associated with immediate lung apoptosis by the up-regulation of the bax protein. J Trauma 49:47–55

de Belder AN, Granath K (1973) Preparation and properties of fluorescein-labelled dextran. Carbohydr Res 30:375–378

Eilig I, Rachinsky M, Artru AA, Alonchin A, Kapuler V, Tarnapolski A, Shapira Y (2001) The effect of treatment with albumin, hetastarch, or hypertonic saline on neurological status and brain edema in a rat model of closed head trauma combined with uncontrolled hemorrhage and concurrent resuscitation in rat. Anesth Analg 92:669–675

Förster H (1989) Pharmacology of hydroxyethyl starch. In: Lawin P, Zander J, Weidler B (eds) Hydroxyethylstärke. Eine aktuelle Übersicht. Springer, Stuttgart, New York, pp 15–27

Förster H, Meier B, Asskali F (1999) Ingestion of fluorescein-labeled hydroxyethyl starch by organ-bound and circulating cells of the reticuloendothelial system. Infusionsther Transfusionsmed 26:45–52

Gall H, Kaufmann R, von Ehr M, Schumann K, Sterry W (1993) Persistent pruritus after hydroxyethyl starch infusions. Retrospective long-term study of 266 cases. Hautarzt 44:713–716

Gall H, Schultz KD, Boehncke WH, Kaufmann R (1996) Clinical and pathophysiological aspects of hydroxyethyl starch-induced pruritus: evaluation of 96 cases. Dermatology 192:222–226

Gavrieli Y, Sherman Y, Ben-Sasson SA (1992) Identification of programmed cell death in situ via specific labeling of nuclear DNA fragmentation. J Cell Biol 119:493–501

Heilmann L (1989) Clinical results after hemodilution with hydroxyethyl starch in pregnancy. Z Geburtshilfe Perinatol 193:219–225

Heilmann L, Lorch E, Hojnacki B, Müntefering H, Förster H (1991) Accumulation of two different hydroxyethyl starch preparations in the placenta after hemodilution in patients with fetal intrauterine growth retardation or pregnancy hypertension. Infusionstherapie 18:236–243

Hulse JD, Jacobi A (1983) An overview of the colloid and its metabolism. Drug Intell Clin Pharmacol 17:334–341

Jurecka W, Szépfalusi Z, Parth E, Schimetta W, Gebhart W, Scheiner O, Kraft D (1993) Hydroxyethylstarch deposits in human skin – a model for pruritus? Arch Dermatol Res 285:13–19

Karinen J, Rasanen J, Paavilainen T, Alahuhta S, Jouppila R, Jouppila P (1994) Uteroplacental and fetal haemodynamics and cardiac function of the fetus and newborn after crystalloid and colloid preloading for extradural caesarean section anaesthesia. Br J Anaesth 73:751–757

Kiesewetter H, Blume J, Jung F, Spitzer S, Wenzel E (1990) Haemodilution with medium molecular weight hydroxyethyl starch in patients with peripheral arterial occlusive disease stage IIb. J Int Med 227:107–114

Kimme P, Jannsen B, Gupta A, Vegfors M (2001) High incidence of pruritus after large doses of hydroxyethyl starch (HES) infusions. Acta Anaesthesiol Surg 45:686–689

Knudson CM, Korsmeyer SJ (1997) Bcl-2 and Bax function independently to regulate cell death. Nat Genet 16:358–363

Kraft D, Sirtl C, Laubenthal H, Scheiner O, Parth E, Dieterich HJ, Szépfalusi Z, Trampisch HJ, Gerlach E, Peter K (1992) No evidence for the existence of preformed antibodies against hydroxyethyl starch in man. Eur Surg Res 24:138–142

Lenz G, Hempel V, Junger H, Werle H, Buckenmaier P (1986) Effect of hydroxyethyl starch, oxypolygelatin and human albumin on the phagocytic function of the reticuloendothelial system in healthy subjects. Anaesthesist 35:423–428

Leunig A, Szeimies RM, Wilmes E, Gutmann R, Stolz W, Feyh J (1995) Clinical and electron microscopy study of sudden deafness treatment with the 10% HES 200/0.5 and pentoxifylline combination. Laryngorhinootologie 74:135–140

Messmer K, Kreimeier U, Intaglietta M (1986) Present state of intentional hemodilution. Eur Surg Res 18:254–263

Metze D, Reimann S, Szepfalusi Z, Bohle B, Kraft D, Luger TA (1997) Persistent pruritus after hydroxyethyl starch infusion therapy: a result of long-term storage in cutaneous nerves. Br J Dermatol 136:553–559

Murphy M, Carmichael AJ, Lawler AJ, White PG, Cox NH (2001) The incidence of hydroxyethyl starch-associated pruritus. Br J Dermatol 144:973–976

Parker NE, Porter JB, Williams HJM, Leftley N (1982) Pruritus after administration of hetastarch. Br Med J 284:385–386

Parth E, Jurecka W, Szépfalusi Z, Schimetta W, Gebhart W, Scheiner O, Kraft D (1992) Histological and immunohistochemical investigations of hydroxyethylstarch deposits in rat tissues. Eur Surg Res 24:13–21

Richter W, Hedin H (1983) Solutions and emulsions used for intravenous infusions. In: Weck AL de, Bungaard H (eds) Handbook of experimental pharmacology, vol. 63. Springer, Berlin Heidelberg New York, pp 581–626

Sakaki T, Tsunoda S, Utsumi S (1990) The influence of volume expansion with induced hypertension on vessel reactivities, the blood-brain barrier, and cerebral infarction in cats with one-hour occlusion of the middle cerebral artery. Neurosurgery 27:268–274

Saling P, Langner K, Saling E, Unger M, Jimenez E, Vogel M (1990) Placental changes after hydroxyethyl starch (HES) infusions. In: Dudenhausen JW (ed) Perinatale Medizin. Thieme, Stuttgart, pp 233–234

Schell RM, Cole DJ, Schultz RL, Osborne TN (1992) Temporary cerebral ischemia. Anesthesiology 77:86–92

Schmelz M (2001) A neuronal pathway for itch. Nat Neurosci 4:8–10

Shatney CH, Chaudry IH (1984) Hydroxyethyl starch administration does not depress reticuloendothelial function or increase mortality from sepsis. Circ Shock 13:21–26

Sirtl C, Laubenthal H, Zumtabel V, Kraft D, Jurecka W (1999) Tissue deposits of hydroxyethyl starch (HES): dose-dependent and time-related. Br J Anaesth 82:510–515

Ständer S, Szépfalusi Z, Bohle B, Ständer H, Kraft D, Luger T, Metze D (2001) Differential storage of hydroxyethyl starch (HES) in the skin: an immunoelectron-microscopical long-term study. Cell Tissue Res 304:261–269

Szeimies RM, Stolz W, Wlotzke U, Korting HC, Landthaler M (1994) Successful treatment of hydroxyethyl starch-induced pruritus with topical capsaicin. Br J Dermatol 131:380–382

Thompson WL, Fukushima T, Rutherford RB, Walton RP (1979) Intravascular persistence, tissue storage and excretion of hydroxyethyl starch. Infusionsther Klin Ernahr 6:151–155

Unger M, Jimenez E, Vogel M, Huang Z, Wagner G, Reichelt A, Saling P, Langner K (1990) Morphological placental changes after hydroxyethyl starch infusions. In: Dudenhausen JW, Saling E (eds) Perinatale Medizin. Thieme, Stuttgart, pp 235–237

White KL, Krasula RW, Munson AE, Holsapple MP (1986) Effects of hydroxyethylstarch (Hespan), a plasma expander, on the functional activity of the reticuloendothelial system. Comparison with human serum albumin and pyran copolymer. Drug Chem Toxicol 9:305–322

Zikria BA, Subbarao C, Oz M, Shih ST, McLeod PF, Sachdev R, Freeman HP, Hardy MA (1989) Macromolecules reduce abnormal microvascular permeability in rat limb ischemia-reperfusion injury. Crit Care Med 17:1306–1309